IEEE Access
Multidisciplinary | Rapid Review | Open Access Journal

Received July 10, 2021, accepted July 19, 2021, date of publication July 26, 2021, date of current version August 2, 2021.

*Digital Object Identifier 10.1109/ACCESS.2021.3099432*

# An Optimal Secondary Multi-Bus Voltage and Reactive Power Sharing Control Based on Non-Iterative Decoupled Linearized Power Flow for Islanded Microgrids

**YI CHYN CASSANDRA WONG[1,2], (Student Member, IEEE), CHEE SHEN LIM[1], (Senior Member, IEEE), HUI HWANG GOH[3], (Senior Member, IEEE), ANDREW CRUDEN[2], MIHAI DRAGOS ROTARU[4], (Member, IEEE), AND XIN KONG[5]**

[1]University of Southampton Malaysia, Iskandar Puteri, Johor 79200, Malaysia
[2]School of Engineering, University of Southampton, Southampton SO17 1BJ, U.K.
[3]School of Electrical Engineering, Guangxi University, Nanning 530015, China
[4]Institute of Microelectronics, Agency for Science, Technology and Research, Singapore 138634
[5]Energy Research Institute at NTU, Nanyang Technological University, Singapore 627590

Corresponding author: Hui Hwang Goh (hhgoh@gxu.edu.cn)

This work was supported in part by the School of Engineering, University of Southampton, U.K., and in part by the School of Electrical Engineering, Guangxi University, China.

**ABSTRACT** The subject of optimal secondary control of power-electronic-interfaced distributed energy resources (DERs) in droop-controlled microgrids has garnered significant research attention in recent years. While the feasibility of optimal secondary control based on non-linear power flow has been proven, the power flow algorithm is essentially iterative in nature. This work proposes an optimal secondary control with non-iterative power flow to regulate multi-bus voltages and DERs' reactive powers. The control scheme incorporates a modified Decoupled Linearized Power Flow that is known to be superior in terms of reactive power and bus voltage magnitude estimation, as compared to classical DC power flow, into a constrained quadratic programming. *Q-V* droop is integrated into the linear power flow in place of the slack bus. The proposed optimal scheme is provably accurate for maintaining reactive power sharing while regulating multiple load-bus voltages. The additional degrees of freedom enabled by the weighting factors significantly improve the control flexibility of the secondary controller. The allowable bus voltages and DER kVar capacity limits have also been considered by the control algorithm. The work is proven through an accurate co-simulation study comprising an 18-bus network and a full primary control models in *PowerFactory*, interfaced through industrial communication tool *MatrikonOPC*.

**INDEX TERMS** Microgrid, droop control, reactive power sharing, voltage regulation, optimal secondary control, decoupled linearized power flow.

## I. INTRODUCTION

Accurate reactive power sharing of distributed energy resources (DERs) in distribution microgrids can be achieved through improved droop schemes based on dispatch mechanisms [1], synchronous-axis voltage droop mechanisms [2], enhanced droop techniques [3], and virtual output impedance (VOI) mechanisms [4], [5]. In applications where bus voltages within the droop-based microgrids are to be regulated concurrently (e.g. being the critical buses or the main points of common coupling with the wider AC grid), advanced secondary voltage control schemes are relevant. In general, these secondary control schemes can be categorized to the types of targeted buses: (i) DER-bus scheme; (ii) load-bus scheme.

In recent years, DER-bus-targeted secondary control schemes for droop-controlled microgrids (i.e. with reactive power sharing correction/control) have been actively

The associate editor coordinating the review of this manuscript and approving it for publication was Shihong Ding.

researched in conjunction with centralized, decentralized, and distributed control structures. Reference [6] adopts a full-graph dispatch droop (with high-bandwidth finite-control-set model predictive voltage controller) to realize average DER-voltage restoration. Reference [7] proposed a non-linear state estimator to realize decentralized secondary DER-voltage control [8]–[14] (with [8] adopting VOI-based primary control) have investigated on consensus-based secondary controls that restore the average DER-voltage while maintaining accurate reactive power sharing. Reference [11] proposed a voltage-consensus scheme to maintain the averaged DER-bus voltage to the rated value. [12], [15] proposed a *PI*-consensus based secondary voltage controller for regulating averaged-DER-bus voltage without the needs of external reference. Different from the typical average-voltage scheme, [16] proposed an observer-based distributed secondary voltage control that can regulate DER voltages to a weighted-average value (while considering constraints on reactive powers). References [13], [14] reported on a tunable consensus control to address the conflicting objectives of multi-DER-bus voltage regulation and reactive power sharing. Reference [17] proposed a consensus-based containment control attempting to keep the DER-bus voltages within upper and lower bounds. Reference [18] proposed and studied a two-layer, iterative consensus control strategy that minimizes overall DER-bus voltage deviation while attempting to maintain accurate reactive power sharing.

On the other hand, load-bus schemes are also relevant. It has been established in [19] that the single load-bus secondary voltage control can be achieved, through *PI*-consensus control, without compromising the accurate sharing of reactive power. However, it was acknowledged in [20] that the reactive power sharing accuracy may be affected if the DER control gains are coupled. In [21], a *PI*-based, two-layer consensus control scheme realizing single load-bus voltage control with intra- and inter-microgrid reactive power sharing correction, was reported. These works, together with previously mentioned works [6]–[14], [16]–[18], have proven that the secondary voltage control with reactive power sharing consideration (of both centralized and non-centralized types) can readily regulate multiple DER-bus and single load-bus voltages. It is also worth noting that some recent works have investigated microgrid's secondary voltage control without emphasizing on reactive power sharing, e.g. single-load-bus-targeted fuzzy-logic-based scheme [22], distributed feedback linearization-approach [23], [24], finite-time distributed control approach [25], and event-triggered-based [26]. Recently, advanced algorithms have been exploited for multi-load-bus voltage regulation. For example, [27] substituted the primary droop-based power control with a neural-network-based control. Reference [28] proposed a multi-objective evolutionary algorithm based on decomposition technique that restores load-bus voltage while considering reactive power sharing.

As far as islanded operating mode is concerned, multi-load-bus voltage regulation schemes embedded with power flow algorithms have also been investigated, e.g. non-linear power flow [29], [30] (which are fitted as non-linear constraints of the optimization problem), Jacobian-based method [31], [32] (specifically, Newton Raphson [33]; Newton-trust region [31]; modified Newton Raphson [32]), neural-network-based non-linear mapping method [34], and virtual-impedance-integrated linear power flow [35]. However, it was learnt that optimal secondary control with non-linear power flow [29], [30] will confront with the issue of slow convergence. This was evidently acknowledged in [29], despite that the work only studied a three-DER network. On the other hand, the convergence issue resulted from the attempt to fit the iterative-based Jacobian power flow into an optimal control problem [33], [34] will aggravate further due to the large number of DERs/buses in future microgrids. On this background, this work sets out to develop an optimal secondary control strategy realizing multi-load-bus voltage and accurate reactive power sharing control, with non-iterative power flow algorithm, for droop-controlled microgrids. (Note: [30], [33] have similar multi-load-bus voltage consideration but have not considered the issue of accurate reactive power sharing, instead, e.g. in [30], network efficiency is considered together).

This work proposes and investigates an optimal secondary control based on modified Decoupled Linearized Power Flow (DLPF) for multi-load-bus voltages and reactive power sharing regulation. Linearized power flow model has always been the preferred algorithm for large-scale power system studies such as contingency analyses and reliability assessments [36], [37]. DLPF was proposed originally in [36] as an alternative to classical DC power flow (which is known to be slightly inferior in terms of bus voltage estimation [36]). In this work, the linear power flow is modified to account for the islanded microgrid's droop control and is then fitted as the linearity constraint of the quadratic programming (QP) problem. Moreover, the allowable voltage and reactive power limits are imposed through the inequality constraints. An 18-bus islanded microgrid has been modelled in detail into *DIgSILENT PowerFactory,* accounting for the primary voltage and current control loops of the power electronic control. The secondary control algorithm is realistically implemented (in terms of communication structure, sampling time and data exchange) in a co-simulated, *Python*-based platform. The secondary controller is interfaced with the network model running in parallel in *PowerFactory* through *MatrikonOPC* – an interoperability standard for data exchange in industrial automation.

The rest of the paper is organized as follows. Section II discusses the fundamentals of network power flow and the DLPF. Section III discusses the aggregation of dispatchable droop control with the DLPF and formulates the constrained QP optimization problem. Section IV details the *PowerFactory-Python* co-simulation platform. Section V investigates the system performance under different practical scenarios such as optimal power sharing, multi-objective optimal power sharing with single/multi-bus

voltage regulation, optimal regulation under voltage and DER capacity limits, as well as communication failure. Section VI discusses and summarizes the main findings and relate them to practical contexts. Section VII concludes the paper.

## II. NETWORK POWER FLOW

### A. BASIC EQUATIONS

A network with $M$ buses can be modelled by forming the network nodal equation

$$\begin{bmatrix} \underset{\sim}{I}_1 \\ \vdots \\ \underset{\sim}{I}_i \\ \vdots \\ \underset{\sim}{I}_M \end{bmatrix} = \begin{bmatrix} \underset{\sim}{Y}_{11} & \cdots & \underset{\sim}{Y}_{1i} & \cdots & \underset{\sim}{Y}_{1M} \\ \vdots & \ddots & \vdots & \ddots & \vdots \\ \underset{\sim}{Y}_{i1} & \cdots & \underset{\sim}{Y}_{ii} & \cdots & \underset{\sim}{Y}_{iM} \\ \vdots & \ddots & \vdots & \ddots & \vdots \\ \underset{\sim}{Y}_{M1} & \cdots & \underset{\sim}{Y}_{M1} & \cdots & \underset{\sim}{Y}_{MM} \end{bmatrix} \times \begin{bmatrix} \underset{\sim}{V}_1 \\ \vdots \\ \underset{\sim}{V}_i \\ \vdots \\ \underset{\sim}{V}_M \end{bmatrix} \quad \text{or} \quad \underset{\sim}{\mathbf{I}} = \underset{\sim}{\mathbf{Y}}\,\underset{\sim}{\mathbf{V}} \tag{1}$$

where the subscript $i$ represents the bus number; and $V_i$ and $I_i$ are the voltage and current injection at $i^{\text{th}}$ bus. $\mathbf{Y}$ is the nodal admittance matrix with its element $Y_{ij} \in \mathbf{Y}$ obtainable from

$$\underset{\sim}{Y}_{ij} = \begin{cases} \underset{\sim}{y}_{i0} + \sum_{\substack{k=1 \\ k\neq 1}}^{M} \underset{\sim}{y}_{ik} & \text{if } i = j \\ -\underset{\sim}{y}_{ij} & \text{othrewise} \end{cases} \tag{2}$$

where $y_{i0}$ is the shunt admittance and $y_{ij}$ is the admittance between bus $i$ and bus $j$ where $y_{ij} = g_{ij} + jb_{ij}$, with $g$ and $b$ being the conductance and susceptance, is the reciprocal of the corresponding complex line impedance $z_{ij}$ $(= r_{ij} + jx_{ij}$, with $r$ and $x$ being the resistance and reactance). Note that any off-diagonal element $Y_{ij}$ is non-zero if and only if there is a branch linking bus $i$ and $j$. If there are $l$ branches in an $M$-bus system then $\mathbf{Y}$ would have $M^2$ elements, of which $(2l + M)$ elements are non-zero.

The current injection at $i^{\text{th}}$ bus can be extracted from (1) as

$$\underset{\sim}{I}_i = \underset{\sim}{Y}_{ii}\,\underset{\sim}{V}_i + \sum_{\substack{j=1 \\ j\neq i}}^{M} \underset{\sim}{Y}_{ij}\,\underset{\sim}{V}_j \tag{3}$$

where the general form of the complex voltage and admittance can be written as $\underset{\sim}{V}_i = V_i\angle\delta_i$ and $\underset{\sim}{Y}_{ij} = Y_{ij}\angle\theta_{ij}$. Then, the apparent power injected at $i^{\text{th}}$ bus can be expressed as [38]

$$\begin{aligned} \underset{\sim}{S}_i &= \underset{\sim}{P}_i + j\,\underset{\sim}{Q}_i = \underset{\sim}{V}_i\,\underset{\sim}{I}_i^{*} \\ &= V_i^2 Y_{ii} e^{-j\theta_{ii}} + V_i \sum_{\substack{j=1 \\ j\neq i}}^{M} V_j Y_{ij} e^{j(\delta_i - \delta_j - \theta_{ij})} \end{aligned} \tag{4}$$

where $Y_{ij} = G_{ij} + jB_{ij}$. Classical iterative techniques such as Gauss-Seidel, Newton-Raphson and fast-decoupled methods are commonly adopted to solve the nonlinear power flow equations. Standard power flow algorithms are not applicable for islanded operation due to two known reasons: the inexistence of slack bus and the dependence of active/reactive power on frequency/voltage due to droop action. In addition, the nonlinearity of basic power flow equations is known for their iterative nature and therefore slow in convergence [36], [39]. Since future microgrids will consist of a significantly large number of DERs (several orders higher than present state of the arts), a more computationally efficient algorithm will be beneficial. Alternatively, the DC power flow algorithm is a convenient option to approximate the linearity between active power injection $P$ and phase angle $\delta$ [37]. However, since it is established based on the assumption of constant bus voltages, reactive power injection is practically neglected [36].

As reported in Fig. 8 of [40], although the classical DC power flow (i.e. Model II in [40]) has the most significant advantages in computational efficiency, computational accuracy is expected to be low in large-area network as voltage magnitude is disregarded. On the other hand, non-iterative DLPF (i.e. Model IV in [40]) exhibits high computational efficiency in term of calculation time compared to the classical AC power flow with accurate voltage magnitude calculation (i.e. Model I in [40]). This provides a basis to this work to evaluate DLPF further in the optimal control algorithm.

### B. DECOUPLED LINEARIZED POWER FLOW ALGORITHM

For microgrids with secondary voltage restoration control, the bus voltage magnitudes are approximately 1.0 pu, i.e. $V_i \approx V_j \simeq 1.0$. The angle difference between the adjacent nodes' voltage phasors tends to remain below 20°, which results in $\cos(\delta_i - \delta_j) \approx 1$ and $\sin(\delta_i - \delta_j) \approx 0$. On this basis, this work adopts a non-iterative, linearized power flow model proposed originally in [36] and [37] (it was known as *Decoupled Linearized Power Flow* (DLPF); mathematical manipulation is detailed in Appendix A, [36] and [37]). Expressing the DLPF in the matrix form, we have

$$\begin{bmatrix} \mathbf{P} \\ \mathbf{Q} \end{bmatrix} = \begin{bmatrix} -\mathbf{B}' & \mathbf{G} \\ -\mathbf{G}' & -\mathbf{B} \end{bmatrix} \begin{bmatrix} \boldsymbol{\delta} \\ \mathbf{V} \end{bmatrix} \tag{5}$$

where $\mathbf{G}$ and $\mathbf{B}$ are the real and imaginary part of the admittance matrix, and $\mathbf{G}'$ and $\mathbf{B}'$ are the corresponding matrices without the shunt element.

## III. MODIFIED DLPF AND QP-BASED OPTIMAL SECONDARY CONTROL

### A. MODIFIED DLFP FOR DROOP-CONTROLLED MICROGRIDS

The active and reactive power injection at $i^{\text{th}}$ bus can be defined as

$$\begin{aligned} P_i &= P_{Li} + P_{Gi} \\ Q_i &= Q_{Li} + Q_{Gi} \end{aligned} \tag{6}$$

where the subscripts $L$ and $G$ represent those of load and generation. Hence, load- and DER-connected buses are hereafter

known as load-bus and droop-bus, respectively. To enable reactive power sharing correction and voltage regulation in an islanded microgrid with $N$ DERs, a dispatch-based $Q-V$ droop scheme is adopted in the primary control with the standard $P-f$ droop control, and are given by

$$\begin{aligned} \omega_i &= \omega_{oi}^* - m_i P_{Gi} \\ V_{Gi} &= V_{oi}^* - n_i Q_{Gi} + u_{com} + n_i Q_{i,dis} \end{aligned} \tag{7}$$

where $\omega_i$ and $V_{Gi}$ are the per-unit operating frequency and the droop voltage amplitude (normalized to network's phase peak voltage) of $i^{\text{th}}$ DER, $\omega_{oi}^*$ and $V_{oi}^*$ are the per-unit no-load frequency and voltage magnitude, $m_i$ and $n_i$ are the per-unit droop coefficients, and $P_{Gi}$ and $Q_{Gi}$ are the filtered per-unit active and reactive output power, normalized to a common base power $S_B$. The reactive power dispatch command $Q_{i,dis}$ of DERs are individually tuned to adaptively adjust the droop voltage amplitude for accurate reactive power sharing. However, since autonomous power sharing is essentially guaranteed by droop control, it is redundant to control all $N$ DERs' $Q_{i,dis}$, instead only ($N$-1) DERs are required (to be elaborated later). Subsequently, a commonly shared voltage correction term $u_{com}$ is introduced to enable network-wide voltage regulation without affecting the reactive power sharing accuracy among the DERs.

From (7), the voltage magnitude at $N$ droop buses can be manipulated in term of reactive power injection $\mathbf{Q}_G$ as

$$\underbrace{\begin{bmatrix} V_{G1} \\ \vdots \\ V_{GN} \end{bmatrix}}_{\mathbf{V}_G} = \underbrace{\begin{bmatrix} V_{o1}^* \\ \vdots \\ V_{oN}^* \end{bmatrix}}_{\mathbf{V}_o^*} - \mathbf{\Phi} \underbrace{\begin{bmatrix} Q_{G1} \\ \vdots \\ Q_{GN} \end{bmatrix}}_{\mathbf{Q}_G} + \mathbf{\Gamma} \underbrace{\begin{bmatrix} u_{com} \\ Q_{1,dis} \\ \vdots \\ Q_{N,dis} \end{bmatrix}}_{\mathbf{u}} \tag{8}$$

where

$$\mathbf{\Phi} = \begin{bmatrix} n_1 & \cdots & 0 & \cdots & 0 \\ \vdots & & \ddots & & \vdots \\ 0 & \cdots & 0 & \cdots & n_N \end{bmatrix}$$

and

$$\mathbf{\Gamma} = \begin{bmatrix} 1 & n_1 & \cdots & 0 \\ \vdots & \vdots & \ddots & \vdots \\ 1 & 0 & \cdots & n_N \end{bmatrix}$$

where $\mathbf{u}$ consists of the common voltage correction term $u_{com}$ and $Q_{i,dis}$ of all DERs. Assumed that the active and reactive power are sufficiently decoupled and knowing that the accurate active power sharing in a droop-controlled islanded microgrid is guaranteed and less affected by the reactive power correction, (5) can be simplified and partitioned (with $\mathbf{Q} = [\mathbf{Q}_L^T \ \mathbf{Q}_G^T]^T$, correspond respectively to reactive power injection at load and droop buses) as

$$\begin{aligned} \begin{bmatrix} \mathbf{Q}_L \\ \mathbf{Q}_G \end{bmatrix}_{k+1} = &- \begin{bmatrix} \mathbf{G'}_{LL} & \mathbf{G'}_{LG} \\ \mathbf{G'}_{GL} & \mathbf{G'}_{GG} \end{bmatrix} \begin{bmatrix} \boldsymbol{\delta}_L \\ \boldsymbol{\delta}_G \end{bmatrix}_{k+1} \\ &- \begin{bmatrix} \mathbf{B}_{LL} & \mathbf{B}_{LG} \\ \mathbf{B}_{GL} & \mathbf{B}_{GG} \end{bmatrix} \begin{bmatrix} \mathbf{V}_L \\ \mathbf{V}_G \end{bmatrix}_{k+1} \end{aligned} \tag{9}$$

By assuming that the load- and droop-buses' steady-state voltage angle remain relatively constant during secondary control, the estimation model for secondary optimization can be determined by replacing $\mathbf{V}_G$ vector in (9) with (8) (detailed manipulation and full expression in Appendix B), expressible as

$$\mathbf{y}(k+1) = \mathbf{C}\mathbf{v}(k) + \mathbf{D}\mathbf{u}(k) \tag{10}$$

with the aid of the measurable sub-vectors $\delta_L$, $\delta_G$ and $\mathbf{Q}_L$, and constant droop parameters, where

$$\begin{aligned} \mathbf{y} &= \begin{bmatrix} \mathbf{V}_L^T & \mathbf{Q}_G^T \end{bmatrix}^T \\ \mathbf{v} &= \begin{bmatrix} \boldsymbol{\delta}_L^T & \boldsymbol{\delta}_G^T & \mathbf{Q}_L^T & \mathbf{V}_o^{*T} \end{bmatrix}^T \\ \mathbf{u} &= \begin{bmatrix} u_{com} & \mathbf{Q}_{dis}^T \end{bmatrix}^T \end{aligned}$$

### B. QUADRATIC PROGRAMMING BASED OPTIMAL SECONDARY CONTROL

The secondary estimation model can be augmented with $\mathbf{u}(k) = \mathbf{u}(k-1) + \Delta\mathbf{u}(k)$ into a standard quadratic programming problem, given by

$$\mathbf{y}(k+1) = \underbrace{\begin{bmatrix} \mathbf{D} & \mathbf{C} \end{bmatrix}}_{\mathbf{F}} \underbrace{\begin{bmatrix} \mathbf{u}(k-1) \\ \mathbf{v}(k) \end{bmatrix}}_{\mathbf{z}(k)} + \mathbf{D}\Delta\mathbf{u}(k) \tag{11}$$

Then, the microgrid voltage regulation and reactive power sharing optimization problem can now be treated as a tracking problem through the following cost function

$$\begin{aligned} J = &\left(\mathbf{y}^*(k+1) - \mathbf{y}(k+1)\right)^T \mathbf{W} \left(\mathbf{y}^*(k+1) - \mathbf{y}(k+1)\right) \\ &+ \Delta\mathbf{u}^T \mathbf{R} \Delta\mathbf{u} \end{aligned} \tag{12}$$

where $\mathbf{y}^*$ is the output setpoint vector. Notably, $\mathbf{W}$ weighting factor enables the possibility of adjusting the priority between reactive power sharing and voltage regulation. On the other hand, $\mathbf{R}$ can adjust the control efforts among $\Delta u_{com}$ and all $\Delta Q_{i,dis}$ in $\Delta\mathbf{Q}_{dis}$. It will be shown that the control objectives of reactive power sharing and multi-bus voltage regulation can be conveniently tuned through $\mathbf{W}$ and $\mathbf{R}$. The cost function (12) of the multi-objective secondary control problem can be formulated into a standard quadratic programming problem, as below:

$$J = \frac{1}{2}\Delta\mathbf{u}^T \mathbf{H} \Delta\mathbf{u} + \Delta\mathbf{u}^T \mathbf{E} \tag{13}$$

where

$$\begin{aligned} \mathbf{H} &= 2\left[\mathbf{D}^T \mathbf{W} \mathbf{D} + \mathbf{R}\right] \\ \mathbf{E} &= -2\mathbf{D}^T \mathbf{W} \left[\mathbf{y}^*(k+1) - \mathbf{F}\mathbf{z}(k)\right] \end{aligned} \tag{14}$$

Apart from the adjustable control priority using weighting factors, network and DER constraints can also be considered in QP (as will be demonstrated in Section V). The most relevant constraints in this control problem are the inequality constraints on the outputs (being the bus voltage limits and the DER reactive power). They can be written as

$$\mathbf{y}_{\min} \le \mathbf{y}(k+1) \le \mathbf{y}_{\max} \tag{15}$$

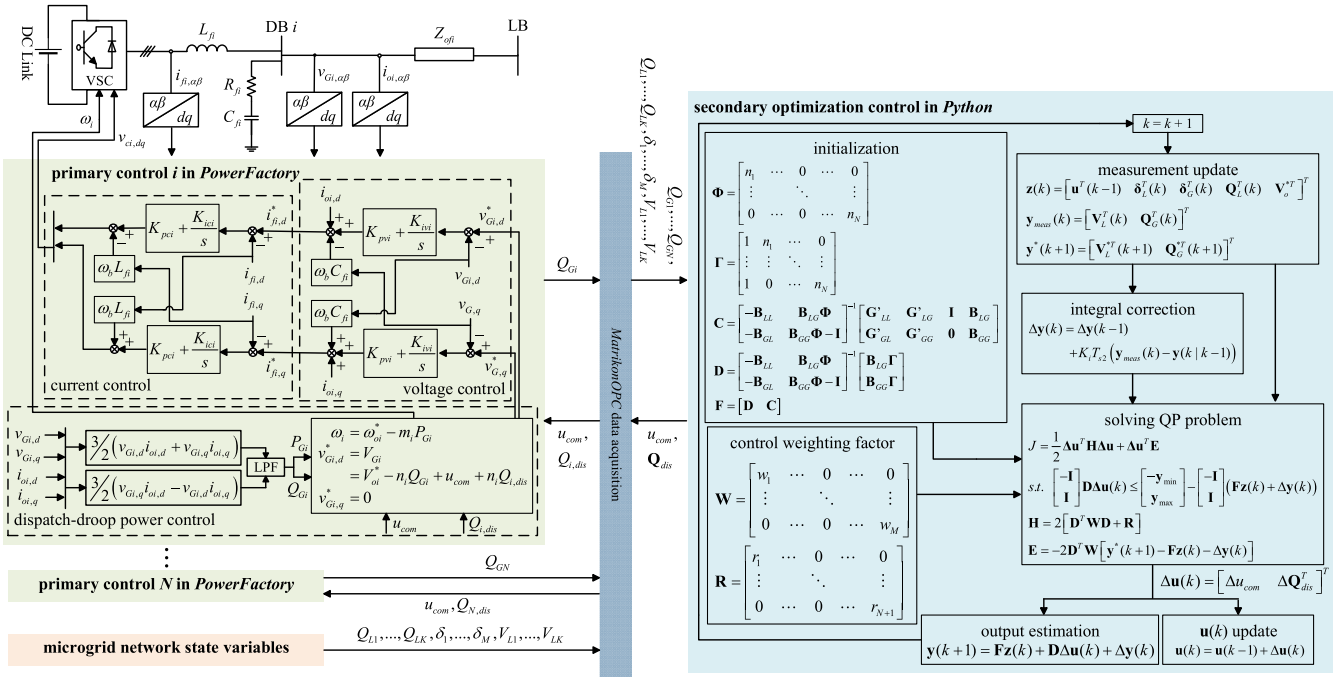


**FIGURE 1.** Detailed block diagram of DER's primary control and the proposed multi-objective optimal secondary control for islanded microgrid.

In order to fit the inequality constraints into the QP formulation, the constraints are decomposed into lower and upper limit [41]

$$\begin{bmatrix} -\mathbf{I} \\ \mathbf{I} \end{bmatrix} \mathbf{y}(k+1) \leq \begin{bmatrix} -\mathbf{y}_{\min} \\ \mathbf{y}_{\max} \end{bmatrix} \tag{16}$$

Based on (11), the inequality constraints can be re-expressed as

$$\begin{bmatrix} -\mathbf{I} \\ \mathbf{I} \end{bmatrix} \mathbf{D}\Delta\mathbf{u}(k) \leq \begin{bmatrix} -\mathbf{y}_{\min} \\ \mathbf{y}_{\max} \end{bmatrix} - \begin{bmatrix} -\mathbf{I} \\ \mathbf{I} \end{bmatrix} \mathbf{F}\mathbf{z}(k) \tag{17}$$

### C. INTEGRAL-BASED CORRECTIVE TERM

The simulation work in Section V (and Fig. 3, in next pages) will show that the adoption of linear power flow (together with associated assumptions) does entail some estimation errors that may be as large as ten percent. This agrees with the general expectation of linear power flow adoption [40], [42]. To improve the estimation, this work subsequently proposes an integral-based corrective term aiming to utilize the available measurements to improve the estimation error. This is done by adding $\Delta\mathbf{y}$ into $\mathbf{y}$ in (11), which gives

$$\Delta\mathbf{y}(k) = \Delta\mathbf{y}(k-1) + K_i T_{s2} \left(\mathbf{y}_{meas}(k) - \mathbf{y}(k|k-1)\right) \tag{18}$$

where $\Delta\mathbf{y}(k)$ is the output estimation error at time $k$, $\mathbf{y}_{meas}$ is the measured output vector, $\mathbf{y}(k|k-1)$ is estimated output vector at time $k-1$ and $K_i$ is the integral gain with the secondary sampling time $T_{s2}$. This expression is somewhat similar to output feedback corrective term which can be found in standard "discrete-time observer". The main difference here is that, instead of system's time dynamics, the optimal control here focuses on real-time dispatch of DERs [43]. The issue of voltage offset has also been identified in other linearized power flow, e.g. [44] where non-integral offset correction technique that is rather computationally intensive (for real-time dispatch problems), is proposed. To incorporate the proposed corrective term into the optimal control, (11), (14) and (17) shall be modified to:

$$\begin{aligned} \mathbf{y}(k+1) &= \mathbf{F}\mathbf{z}(k) + \mathbf{D}\Delta\mathbf{u}(k) + \Delta\mathbf{y}(k) \\ \mathbf{E} &= -2\mathbf{D}^T\mathbf{W}\left[\mathbf{y}^*(k+1) - \mathbf{F}\mathbf{z}(k) - \Delta\mathbf{y}(k)\right] \\ \begin{bmatrix} -\mathbf{I} \\ \mathbf{I} \end{bmatrix} \mathbf{D}\Delta\mathbf{u}(k) &\leq \begin{bmatrix} -\mathbf{y}_{\min} \\ \mathbf{y}_{\max} \end{bmatrix} - \begin{bmatrix} -\mathbf{I} \\ \mathbf{I} \end{bmatrix} (\mathbf{F}\mathbf{z}(k) + \Delta\mathbf{y}(k)) \end{aligned} \tag{19}$$

## IV. POWERFACTORY-PYTHON CO-SIMULATION PLATFORM

A *PowerFactory-Python* co-simulation platform has been established to investigate the proposed optimal secondary control scheme. *MatrikonOPC* is used as the OPC server to facilitate the data acquisition and transfer between the two software instances (being the clients, through *ComLink* and *OpenOPC* interfaces, respectively). The primary control of a DER and the proposed secondary control is detailed in Fig. 1. The primary controller of each DER is modelled entirely from basic block models of sampling clock, sample-and-hold, $\alpha\beta$-$dq$ transformation, and etc.

The default voltage and current measurement in *PowerFactory* is in the $\alpha\beta$ reference frame. The entire primary control is comprised of a dispatch-droop power control, output voltage control and an inverter current control - all are performed in the $dq$ reference frame. The DER output voltage vector is

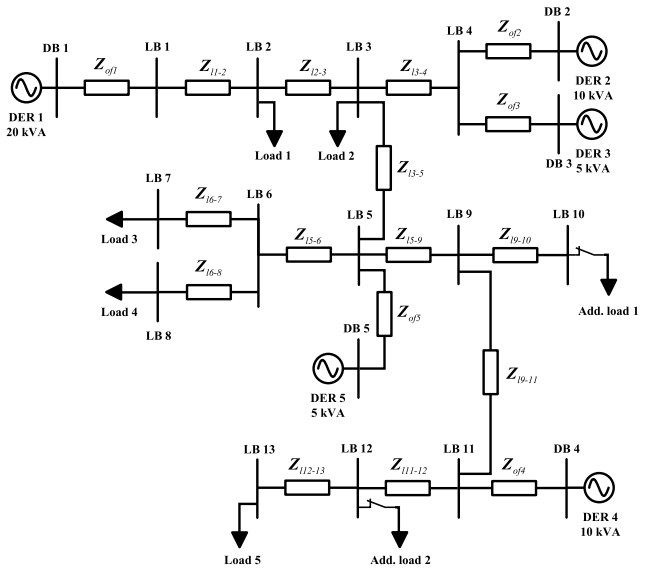


**FIGURE 2.** Single-line diagram of the islanded microgrid test system.

aligned to its synchronous reference frame, as shown below

$$v^*_{Gi,d} = V^*_{oi} - n_i Q_{Gi} + u_{com} + n_i Q_{i,dis}$$
$$v^*_{Gi,q} = 0 \tag{20}$$

The $d$-axis reference is the reference for the inner voltage control loop. The primary voltage and current control are controlled by *PI* controllers, which are tuned in such a way that the control bandwidths are decoupled and the voltage control dynamic having higher bandwidth than the dispatch-droop power control. The tuning steps can be briefly described as follows: the innermost current control loop is tuned first with the assumption of a constant current reference (i.e., typically being the output of voltage control loop), followed by the tuning of voltage controller by assuming a constant output voltage reference (i.e., normally being the output of droop-based power control). The design details are depicted in Fig. 1 but interested readers may also refer to [45], [46] for details.

As for the secondary controller in *Python*, live information such as reactive powers, load-bus voltages, etc., are facilitated through *MatrikonOPC*. Note that in actual implementation some of the state information may be obtained from network state estimation instead of direct measurement. This subject is beyond the focus of the current work hence all state information is obtained directly from the co-simulated network model (Fig. 2) in *PowerFactory*. Each measurement is configured with an OPC tag in *PowerFactory* and is updated to the OPC server at a preset interval while the secondary control reads from the server at a regular period $T_{s2}$ $(= 1/F_{s2})$. Note that the proposed optimal secondary control is designed with prerequisite information such as the constant droop parameters and the network **G**' and **B** matrices. Upon successful iterations of QP (set to a maximum of 100 iterations in the CVXOPT solver) in each control cycle, provided that $\Delta\mathbf{u}(k)$ is greater than a pre-defined minimum threshold (being a very small value), the optimal droop dispatch input **u**, i.e. $u_{com}$ and all $Q_{i,dis}$, will be updated based on $\mathbf{u}(k) = \mathbf{u}(k-1) + \Delta\,\mathbf{u}(k)$.

It is worth noting that the investigation is conducted through the comprehensively developed co-simulation platform, which can be regarded as a "software-in-the-loop" technique. The accuracy of the co-simulation is supported by the state-of-the-art network and DER's primary closed-loop control modelling in *PowerFactory*, and the interoperability data-exchange industrial standard *MatrikonOPC*.

**TABLE 1.** Specifications of the islanded microgrid network and proposed control.

| Parameter | Value | Parameter | | Value |
|---|---|---|---|---|
| Sw. freq. $F_{s1}$ | 2.5 kHz | Primary voltage control | $K_{pvi}$ | 1.23 |
| System freq. | 50 Hz | | $K_{ivi}$ | 4.67 |
| Inverter DC bus | 1 kV | Primary current control | $K_{pci}$ | 0.27 |
| AC voltage levels | 400 V | | $K_{ici}$ | 1.61 |

| DER ratings: Apparent pow. (rated *pf*) | | *P-f* droop coefficients (pu) | *Q-V* droop coefficients (pu) |
|---|---|---|---|
| DER 1 | 20 kVA (0.8) | 0.0625 | 0.075 |
| DER 2 | 10 kVA (0.8) | 0.125 | 0.15 |
| DER 3 | 5 kVA (0.8) | 0.25 | 0.30 |
| DER 4 | 10 kVA (0.8) | 0.125 | 0.15 |
| DER 5 | 5 kVA (0.8) | 0.25 | 0.30 |

| Inverter filter impedances: *L-R*C | | DER output feeder impedances | |
|---|---|---|---|
| $Z_{f1}$ | 7.62 mH, 10 Ω, 3.32 μF | $Z_{of1}$ | 0.03 Ω, 0.35 mH |
| $Z_{f2}$ | 15.24 mH, 10 Ω, 1.66 μF | $Z_{of2}$ | 0.02 Ω, 0.45 mH |
| $Z_{f3}$ | 30.48 mH, 10 Ω, 0.83 μF | $Z_{of3}$ | 0.06 Ω, 0.35 mH |
| $Z_{f4}$ | 15.24 mH, 10 Ω, 1.662μF | $Z_{of4}$ | 0.05 Ω, 0.56 mH |
| $Z_{f5}$ | 30.48 mH, 10 Ω, 0.83 μF | $Z_{of5}$ | 0.03 Ω, 0.42 mH |

| Line impedances | | | |
|---|---|---|---|
| $Z_{l1\text{-}2}$ | 0.21 Ω, 1.50 mH | $Z_{l6\text{-}8}$ | 0.31 Ω, 2.98 mH |
| $Z_{l2\text{-}3}$ | 0.26 Ω, 1.93 mH | $Z_{l5\text{-}9}$ | 0.14 Ω, 1.03 mH |
| $Z_{l3\text{-}4}$ | 0.70 Ω, 3.70 mH | $Z_{l9\text{-}10}$ | 0.10 Ω, 0.54 mH |
| $Z_{l3\text{-}5}$ | 0.28 Ω, 1.76 mH | $Z_{l9\text{-}11}$ | 0.21 Ω, 0.78 mH |
| $Z_{l5\text{-}6}$ | 0.12 Ω, 1.18 mH | $Z_{l11\text{-}12}$ | 0.47 Ω, 3.21 mH |
| $Z_{l6\text{-}7}$ | 0.19 Ω, 2.01 mH | $Z_{l12\text{-}13}$ | 0.16 Ω, 3.06 mH |

| Proposed optimal secondary control | | | |
|---|---|---|---|
| Parameter | Value | Parameter | Value |
| Sampling freq. $F_{s2}$ | 0.2 Hz | LPF time constant $\tau_{c,pq}$ | 0.2 s |
| Integral gain $K_i$ | 0.02 | LPF time constant $\tau_{c,v}$ | 0.9 s |

## V. RESULTS

Fig. 2 depicts the single-line diagram of the microgrid network. The co-simulated network has 5 DERs (3 is used in [29]) and 18 buses – these settings are chosen in order to limit the wait time due to computational burden encountered (owing to the use of detailed primary control loops) when running the network model in a standard computing workstation. The DER specification are tabulated in Table 1 along with primary control (refer to [46] and [47] for details) and secondary control (e.g. $F_{s2}$, $K_i$, etc.) parameters. The power and voltage readings are low-pass filtered at time constants of $\tau_{c,pq}$ and $\tau_{c,v}$, respectively, before being deployed into the secondary control algorithm (in *Python*). DER 1 at droop bus 1 (i.e. DB 1 in Fig. 2) is taken as the reference unit.

In the QP optimization, the weighting factor **W** is a $M$-by-$M$ (i.e. $M = K+N$) diagonal matrix having the form of

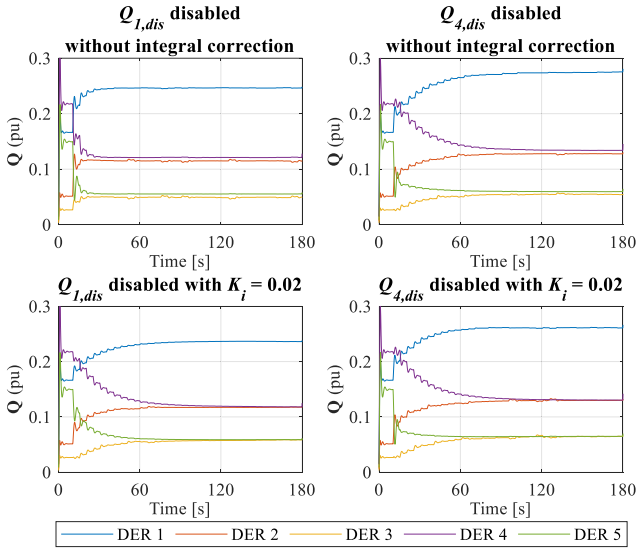


**FIGURE 3.** Optimal reactive power sharing control with and without integral-based error correction: DER reactive output power.

**TABLE 2.** Steady state estimation error (absolute percentage) without/with integral correction.

| | $Q_{1,dis}$ disabled [%] | | $Q_{4,dis}$ disabled [%] | |
|---|---|---|---|---|
| | $K_i = 0$ | $K_i = 0.02$ | $K_i = 0$ | $K_i = 0.02$ |
| DER 1 | **0.00** | **0.00** | 2.69 | 0.23 |
| DER 2 | 8.84 | 0.13 | 4.94 | 0.00 |
| DER 3 | 22.32 | 0.23 | 23.25 | 0.40 |
| DER 4 | 1.23 | 0.13 | **0.00** | **0.00** |
| DER 5 | 11.32 | 0.23 | 12.45 | 0.40 |

diag($w_1, w_2, \ldots . w_M$). $K$ is the number of load-bus (labelled as LB in Fig. 2) and $N$ is the number of DERs. In this work with $K = 13$ and $N = 5$, the individual $w$ weighting factors essentially correspond to outputs $V_{L1}, \ldots, V_{LK}$, $Q_{G1}, \ldots$, and $Q_{GN}$, respectively. Penalty factor $\mathbf{R}$ is a $(N + 1)$-by-$(N + 1)$ diagonal matrix of the form diag($r_1, r_2, \ldots r_{N+1}$). Similarly, the individual $r$ penalty factors correspond, respectively, to control inputs $\Delta u_{com}$, $\Delta Q_{1,dis}, \ldots$, and $\Delta Q_{N,dis}$.

Fig. 3 first demonstrates the effectiveness of the proposed error correction technique (as explained in Section III-C) in mitigating errors due to power flow linearization. Before introducing (18)-(19), the reactive power sharing remains slightly non-proportional, in pu (with respect to their ratings, Table 1); upon correction with $K_i = 0.02$, they are restored to the proportional ratio of 4:2:1:2:1 (Fig. 3). The absolute percentage estimation error is tabulated in Table 2 with DER 1 acted as the reference for the case "$Q_{1,dis}$ disabled" and vice versa. The slight difference in individual reactive output powers (between the "$Q_{1,dis}$ disabled" and "$Q_{4,dis}$ disabled" cases) is due to the voltage-dependent nature of the loads.

Next, the secondary control scheme in conjunction with different control settings is investigated. By default, a total passive load of 15 kW and 9 kVar are present in the islanded microgrid. Additional loads are connected to LB 10 and LB 12 at a chosen simulation time instant, upon which, the total load demand increases to $22 + j13$ kVA.

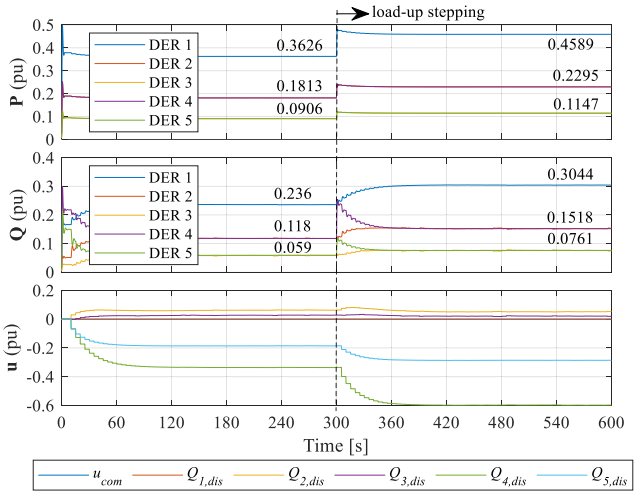


**FIGURE 4.** Case A: Optimal reactive power sharing control: DERs active/reactive output power and secondary control input u.

### A. OPTIMAL SHARING OF REACTIVE POWER

Initially, the DERs are controlled through the standard droop control without the proposed secondary control. It can be established from Fig. 4 that while the active power is always proportionally shared, the reactive power is not. As explained in Section III-A, it is redundant to utilize all $N$ DERs' $Q_{i,dis}$ for reactive power sharing correction control, instead only those for ($N$-1) DERs are required. Hence, the $r_i$ value of a DER should be set significantly large (DER 1 is chosen in subsequent studies).

At $t = 10$ s, the proposed optimal secondary control layer with deactivated voltage regulation (achieved by setting $w_{14} - w_{18}$ to 10) is started. Penalty factor $\mathbf{R}$ is set to diag(10$e$10, 10$e$10, 5, 5, 5, 5), which essentially activates $Q_{2,dis}$ to $Q_{5,dis}$ for reactive power sharing correction. The reactive power sharing among the DERs (with $K_i = 0.02$) is significantly improved, giving the ratio of 4:2:1:2:1 at steady state. The corresponding voltages of the droop- and load-buses are shown in Fig. 5, ranging from 0.9132 pu (i.e., LB 13) to 1.0112 pu (i.e., DB 2). Subsequently, additional loads are connected to LB 10 and LB 12 at (approx.) $t = 300$ s. Figs. 4-5 show that proportional reactive power sharing can be retained by the proposed control even after load increase, with the minimum and maximum voltage magnitudes being $V_{L13} = 0.8584$ pu and $V_{G2} = 1.0027$ pu.

### B. SINGLE LOAD-BUS VOLTAGE REGULATION

The islanded microgrid is loaded with the default loadings, and the voltage magnitude at LB 12, $V_{L12}$ has "drooped" to 0.9584 pu. At $t = 10$ s, the proposed control is activated with $w_{12}$ (corresponds to $V_{L12}$) set to 10, and others set to zero (which means the reactive power control is deactivated). $\mathbf{R}$ is set as diag(10, 10$e$10, 10$e$10, 10$e$10, 10$e$10, 10$e$10), which

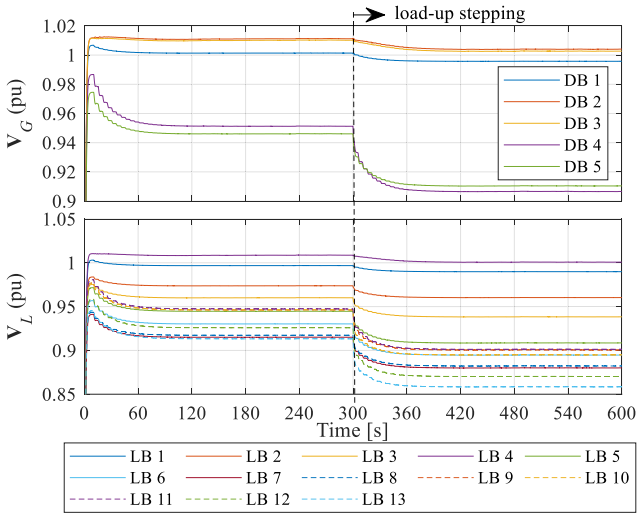


**FIGURE 5.** Case A: Optimal reactive power sharing control: DER droop voltage magnitudes and load-bus voltage magnitudes.

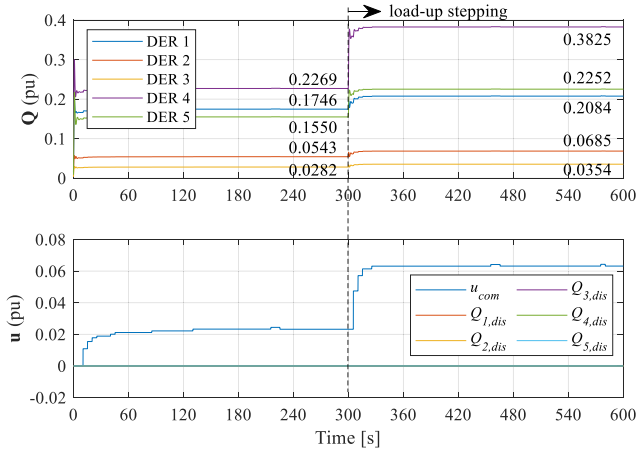


**FIGURE 6.** Case B: Single load bus voltage regulation control: DERs reactive output power and secondary control input u.

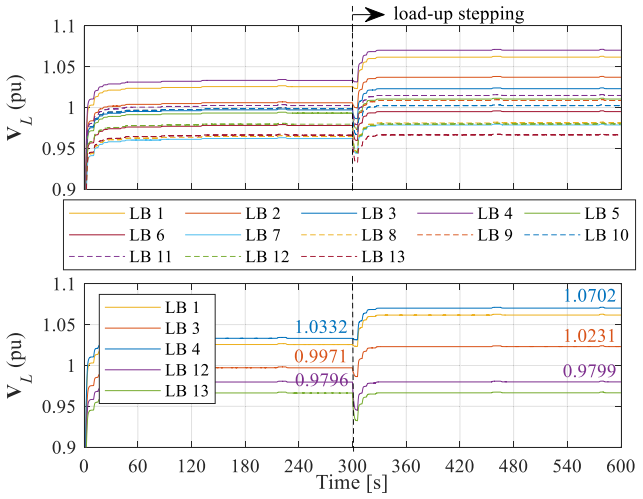


**FIGURE 7.** Case B: Single load bus voltage regulation control: load-bus voltage magnitudes.

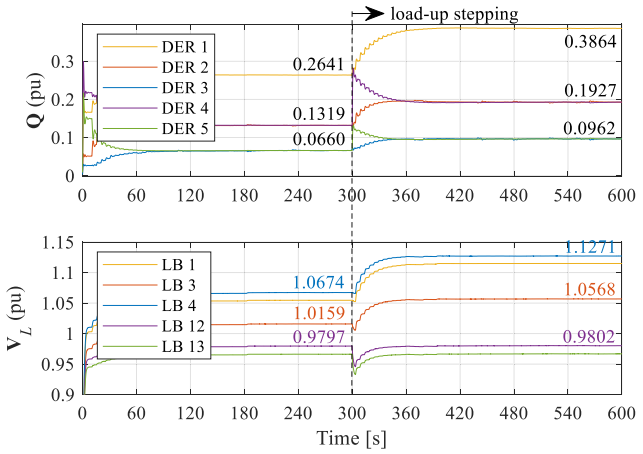


**FIGURE 8.** Case C: Optimal reactive power sharing and single load-bus voltage regulation control: reactive output power and load-bus voltage magnitudes.

means only $u_{com}$ is activated. It can be clearly seen from Figs. 6 and 7 that $V_{L12}$ is regulated to $V^{ref} = 0.98$ pu through adjustment of the voltage correction term $u_{com}$ without any noticeable transient in the DERs' reactive output power. Upon loads up-stepping at $t = 300$ s, the voltage magnitude at load-bus LB 12 is retained at 0.98 pu but the issue of non-proportional reactive power sharing persists, as expected.

### C. OPTIMAL REACTIVE POWER SHARING AND VOLTAGE REGULATION

The case of simultaneous optimal reactive power sharing and voltage regulation is investigated next. Initially, the DERs are allowed to droop at the default load condition. At $t = 10$ s, the optimal secondary control is activated by setting $\mathbf{W}$ as $w_{12}, w_{14} - w_{18} = 10$ and $\mathbf{R}$ as diag(10, 10$e$10, 5, 5, 5, 5). Fig. 8 shows, despite loads up-stepping (at $t = 300$s), proportional reactive power sharing can be achieved among the DERs and $V_{L12}$ is always regulated to $V^{ref} = 0.98$ pu. This confirms the viability of the proposed optimal secondary control for the case with single load-bus.

Next, the performance of optimal reactive power sharing and multi-load-buses voltage regulation is examined. At default loading condition, the voltage magnitude at LB 12 is of 0.9584 pu with $V_{L4} = 1.0104$ pu. In case C-I, multi-load-buses voltage regulation control is prioritized but with an emphasis on reactive power sharing improvement. At $t = 10$ s, the proposed control is activated by setting $\mathbf{W}$ with $w_{12} = 100$ and $w_{14} - w_{18} = 10$, and $\mathbf{R}$ as diag(10, 10$e$10, 5, 5, 5, 5).

Subsequently, at $t = 300$ s, $w_4$ is changed from 0 to 100 in order to realize multi-bus voltage ($V_{L4}$ and $V_{L12}$) regulation. Fig. 9 clearly demonstrates the trade-offs between optimal reactive power sharing among the DERs and multi-bus voltage regulation. Precise single-bus voltage regulation (i.e. $V_{L12}$ be regulated to $V_{L12}^{ref} = 0.98$ pu) and proportional reactive power sharing are achieved before 300 s. Upon

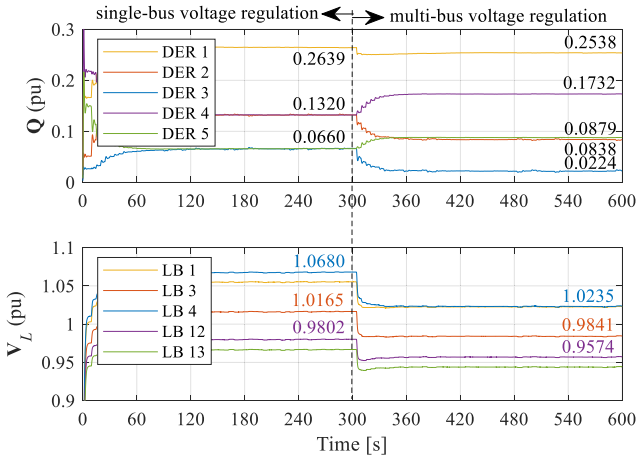


**FIGURE 9.** Case C-I: Optimal reactive power sharing and prioritized multi-load-bus voltage regulation control: DERs reactive output power and load-bus voltage magnitudes.

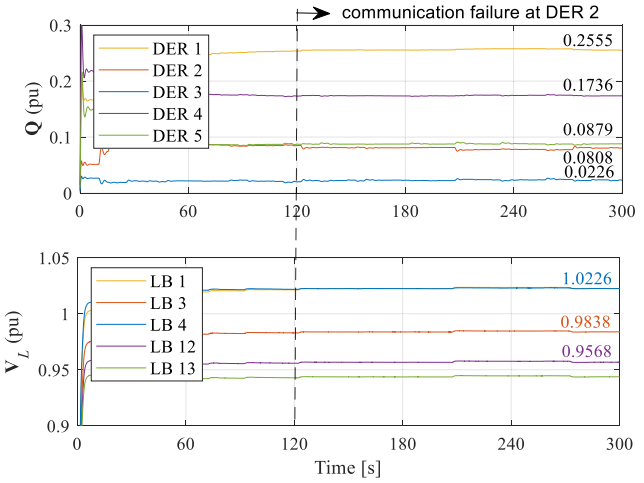


**FIGURE 10.** Case C-II: Optimal reactive power sharing and multi-load-bus voltage regulation control with communication failure: DERs reactive output power and load-bus voltage magnitudes.

the multi-load-bus voltage regulation (i.e. $V_{L4}^{ref} = 1.0$ pu), although $V_{L4}$ and $V_{L12}$ are both regulated close to their references (1.0235 pu and 0.9574 pu), proportional reactive power sharing is compromised. This is because $\mathbf{W}$ weighs voltage regulation heavier than reactive power sharing (100 vs 10).

The robustness of the proposed optimal control against communication failure is examined next in case C-II. Specifically, DER 2 is chosen as the subject, and the "communication failure" is realistically simulated by "freezing" the communication in and out of DER 2, leaving DER 2 to operate under droop control with fixed dispatch commands. The proposed control is activated with multi-bus voltage regulation and reactive power sharing at $t = 10$ s. Weighting/penalty factors $\mathbf{W}$ and $\mathbf{R}$ are set the same as that in case C-I. Communication in and out of DER 2 are lost at $t = 120$ s and the optimal controller retains the last available DER 2's reactive power. As shown in Fig. 10, the reactive power ratio and bus voltages have been slightly affected after 120 s (until 300 s), as compared to the result in case C-I (Fig. 9). This result nevertheless confirms the robustness of the proposed optimal control towards communication loss even for a sustained period. In practical scenarios, communication loss is usually detected (and mitigated) in a much shorter time duration.

In scenario C-III, both the voltage regulation and reactive power sharing are weighted equally (by setting $w_4$, $w_{12}$, $w_{14} - w_{18}$ to 10) with $\mathbf{R}$ remains as diag(10, 10$e$10, 5, 5, 5, 5). It can be clearly seen from Fig. 11 that the reactive power sharing error among the DERs is significantly improved (ratio as shown in Fig. 11) while $V_{L4}$ and $V_{L12}$ are more loosely regulated.

### D. CONSTRAINED OPTIMAL REACTIVE POWER SHARING AND MULTI-BUS VOLTAGE REGULATION

Next, the ability of the QP-based secondary control in dealing with limits (by activating the inequality constraints (19)) is examined. The islanded microgrid is loaded with the default

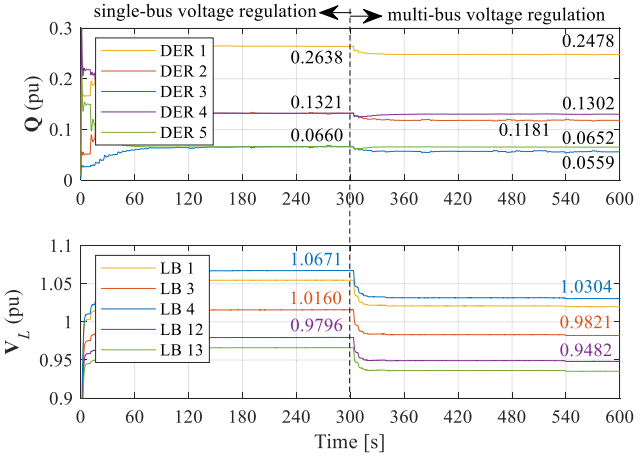


**FIGURE 11.** Case C-III: Optimal reactive power sharing and multi-load-bus voltage regulation control: DERs reactive output power and load-bus voltage magnitudes.

loading and at $t = 10$ s, the secondary control with equal weighting of voltage regulation and reactive power sharing, is activated. Weighting/penalty factors $\mathbf{W}$ and $\mathbf{R}$ are set the same as scenario C-III and LB 3 is selected as a critical bus with the desire to achieve a voltage tolerance of $\pm 1\%$ (and with the DERs reactive output power limited to their respective capacity limit; the remaining buses are limited loosely to $-6\%/+10\%$ from 1.0 pu). It can be seen from Fig. 12 that, while $V_{L12}$ is regulated to 0.9738 pu (with $V_{L12}^{ref} = 0.98$ pu) and the reactive power sharing ratio is improved to 0.2608:0.1312:0.0654, the unregulated $V_{L3}$ (since $w_3 = 0$) is maintained at 1.01 pu (as opposed to the unconstrained scenario in case C-III, $V_{L3} = 1.016$ pu, as in Fig. 11). Then, at $t = 300$ s, multi-bus voltage regulation is activated by setting $w_4$ as 10 (i.e., activating $V_{L4}$ regulation with $V_{L4}^{ref} = 1.0$ pu). It is shown that the proposed QP-based optimal control can regulate $V_{L4}$ and $V_{L12}$ to, respectively, 1.038 pu and 0.9556 pu, and maintain near-proportional reactive power sharing. Voltage of the critical bus LB 3 is kept at approximately 0.99 pu.

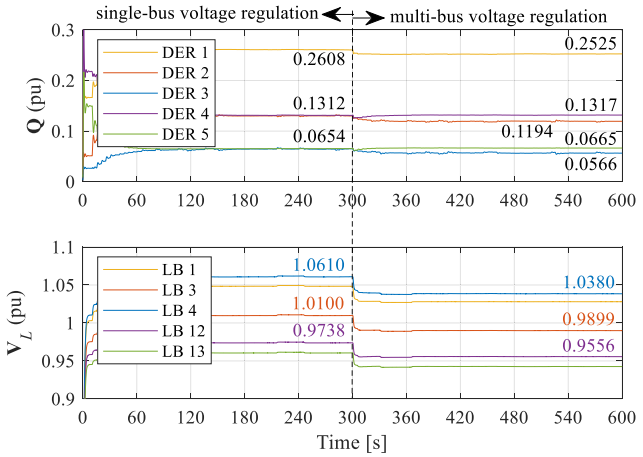


**FIGURE 12. Case D: Constrained optimal reactive power sharing and multi-load-bus voltage regulation control: DERs reactive output power and load-bus voltage magnitudes.**

This result fully demonstrates the capability of the QP-based multi-objective optimal secondary control in considering the network constraints.

## VI. DISCUSSION

In the preceding sections, the optimal secondary control has been tested in conjunction with three distinctive cases: reactive power sharing correction without voltage regulation, single-load bus voltage regulation without reactive power sharing correction, and lastly, optimal reactive power sharing and single-/multi-bus voltage regulation. These results have verified the performance of the proposed optimal control in handling the intrinsic trade-offs between reactive power sharing and voltage regulation in droop-controlled islanded microgrids. The ability of the proposed QP-based secondary control in handling practical constraints is also fully verified. The load-bus voltage and DERs' reactive power limits consideration are practically relevant to the scenarios of critical buses and physically limited kVA capacities of e.g. grid battery system (being a dispatchable DER).

Possible applications of the proposed control strategy include but not limited to the following: the single load-bus voltage regulation is relevant to the context of synchronizing the islanded microgrid's point of interconnection with the wider AC grid, specifically, during the transition from islanded mode to grid-connected mode; for islanded microgrids with multiple critical/sensitive buses, apart from maintaining a fairly accurate reactive power sharing (means whenever physically possible) among the DERs, the multi-bus voltage regulation will be useful in keeping the voltage magnitude of those critical buses within the desired limits, either through the direct voltage regulation feature or the constraint-handling feature of the optimal secondary controller.

Lastly, discussion on the relevance of extending the proposed control scheme for frequency regulation, e.g. [48], and power oscillation, e.g. [49], [50], is due. Frequency regulation/restoration can be readily achieved (in either central or distributed manner) by correcting the frequency droop deviation through a modified $P-f$ droop equation in (7). On the other hand, if one intends to improve the active power oscillation, the common approach is through the intervention at the primary control [49], [50], owing to the control bandwidth requirement. Therefore, the proposed DLPF-based optimal secondary control (even after augmenting it to include active-power-frequency droop) is likely not suitable for these purposes.

## VII. CONCLUSION

In this paper, we propose a non-iterative based multi-objective optimal secondary control scheme based on modified Decoupled Linearized Power Flow to address the control objectives with intrinsic trade-off: optimal reactive power sharing among DERs and voltage regulation at multiple load-buses in droop-controlled islanded microgrids. The constrained secondary control is framed into a generic QP problem with linear constraints to enable the deployment of established solver, e.g. CVXOPT. The proposed secondary control not only capable to realize single-objective control, i.e. optimal reactive power sharing or single-bus voltage regulation, it can also accomplish multi-objective control, e.g. single load-bus voltage regulation and optimal reactive power sharing without compromising proportional reactive power sharing. The control scheme can also optimally regulate multiple load-bus voltages with tradeoffs of reactive power sharing. It is provably capable to keep the network variables, e.g. load-bus voltages and DERs' reactive power outputs, to within the predefined limits. The priority among the output objectives and control efforts can also be flexibly adjusted through weighting and penalty factors (being $\mathbf{W}$ and $\mathbf{R}$ here). All the claims have been supported by theoretical derivation and substantiated with extensive simulation proofs.

Lastly, for future works, the proposed non-iterative based optimal secondary control scheme should be benchmarked against relevant control techniques, e.g., iterative-based counterpart. Moreover, in order to alleviate the risk of single-point failure of centralized control and ease the computational load of the optimal control strategy, the next logical step is to develop the optimal secondary control scheme into a distributed architecture.

## APPENDIX A
## DECOUPLED LINEARIZED POWER FLOW ALGORITHM

The terms $\mathbf{B}$, $\mathbf{B}'$, $\mathbf{G}$ and $\mathbf{G}'$ in (8) can be extracted from the following expressions (see [36] for detailed steps):

$$\begin{aligned} P_i &= V_i^2 G_{ii} + \sum_{\substack{j=1 \\ j\neq i}}^{M} V_i V_j \left[B_{ij}\sin\left(\delta_i-\delta_j\right)+G_{ij}\cos\left(\delta_i-\delta_j\right)\right] \\ &= V_i^2 G_{ii} + \sum_{\substack{j=1 \\ j\neq i}}^{M} V_i V_j \left[B_{ij}\sin\Delta\delta_{ij}+G_{ij}\cos\Delta\delta_{ij}\right] \\ &= V_i^2 G_{ii} + \sum_{\substack{j=1 \\ j\neq i}}^{M} V_i V_j \left[B_{ij}\Delta\delta_{ij}+G_{ij}\right] \\ &= \sum_{j=1}^{M} G_{ij}V_j - \sum_{j=1}^{M} B'_{ij}\delta_j \end{aligned} \tag{21}$$

$$
\begin{aligned}
Q_i &= -V_i^2 B_{ii} + \sum_{\substack{j=1 \\ j\neq i}}^{M} V_i V_j \left[G_{ij} \sin\left(\delta_i - \delta_j\right) - B_{ij} \cos\left(\delta_i - \delta_j\right)\right] \\
&= -V_i^2 B_{ii} + \sum_{\substack{j=1 \\ j\neq i}}^{M} V_i V_j \left[G_{ij} \sin \Delta\delta_{ij} - B_{ij} \cos \Delta\delta_{ij}\right] \\
&= -V_i^2 B_{ii} + \sum_{\substack{j=1 \\ j\neq i}}^{M} V_i V_j \left[G_{ij} \Delta\delta_{ij} - B_{ij}\right] \\
&= -\sum_{j=1}^{M} B_{ij} V_j - \sum_{j=1}^{M} G'_{ij} \delta_j
\end{aligned} \tag{22}
$$

## APPENDIX B
## SECONDARY ESTIMATION MODEL IN (10)

DER-bus voltage terms in (8) are substituted into (9) to express $\mathbf{V}_G$ in terms of reactive power injection, constant droop parameters, and control inputs $\mathbf{u}$, i.e., $u_{com}$ and $\mathbf{Q}_{dis}$, with the assumption that the steady-state voltage angle $\delta$ (obtainable from measurement) remain relatively constant during the secondary control adjustment. This gives

$$
\begin{aligned}
&\begin{bmatrix} -\mathbf{B}_{LL} & \mathbf{B}_{LG}\mathbf{\Phi} \\ -\mathbf{B}_{GL} & \mathbf{B}_{GG}\mathbf{\Phi} - \mathbf{I} \end{bmatrix} \underbrace{\begin{bmatrix} \mathbf{V}_L \\ \mathbf{Q}_G \end{bmatrix}_{k+1}}_{\mathbf{y}(k+1)} \\
&= \begin{bmatrix} \mathbf{G'}_{LL} & \mathbf{G'}_{LG} & \mathbf{I} & \mathbf{B}_{LG} \\ \mathbf{G'}_{GL} & \mathbf{G'}_{GG} & \mathbf{0} & \mathbf{B}_{GG} \end{bmatrix} \underbrace{\begin{bmatrix} \boldsymbol{\delta}_L \\ \boldsymbol{\delta}_G \\ \mathbf{Q}_L \\ \mathbf{V}_o^* \end{bmatrix}_k}_{\mathbf{v}(k)} \\
&\quad + \begin{bmatrix} \mathbf{B}_{LG}\mathbf{\Gamma} \\ \mathbf{B}_{GG}\mathbf{\Gamma} \end{bmatrix} \underbrace{\begin{bmatrix} u_{com} \\ Q_{1,dis} \\ \vdots \\ Q_{N,dis} \end{bmatrix}_k}_{\mathbf{u}(k)}
\end{aligned} \tag{23}
$$

By re-assembling the known sub-vectors, i.e. $\delta_L$, $\delta_G$, $\mathbf{Q}_L$ and $\mathbf{V}_o^*$, into a single vector $\mathbf{v}$, one can obtain (10), where $\mathbf{C}$ is a $M \times 2M$ matrix and $\mathbf{D}$ is a $M \times (N+1)$ matrix, which can be expressed as

$$
\mathbf{C} = \begin{bmatrix} -\mathbf{B}_{LL} & \mathbf{B}_{LG}\mathbf{\Phi} \\ -\mathbf{B}_{GL} & \mathbf{B}_{GG}\mathbf{\Phi} - \mathbf{I} \end{bmatrix}^{-1} \begin{bmatrix} \mathbf{G'}_{LL} & \mathbf{G'}_{LG} & \mathbf{I} & \mathbf{B}_{LG} \\ \mathbf{G'}_{GL} & \mathbf{G'}_{GG} & \mathbf{0} & \mathbf{B}_{GG} \end{bmatrix}
$$

$$
\mathbf{D} = \begin{bmatrix} -\mathbf{B}_{LL} & \mathbf{B}_{LG}\mathbf{\Phi} \\ -\mathbf{B}_{GL} & \mathbf{B}_{GG}\mathbf{\Phi} - \mathbf{I} \end{bmatrix}^{-1} \begin{bmatrix} \mathbf{B}_{LG}\mathbf{\Gamma} \\ \mathbf{B}_{GG}\mathbf{\Gamma} \end{bmatrix}
$$

## REFERENCES


[1] H. Mahmood, D. Michaelson, and J. Jiang, "Reactive power sharing in islanded microgrids using adaptive voltage droop control," *IEEE Trans. Smart Grid*, vol. 6, no. 6, pp. 3052–3060, Nov. 2015.

[2] R. M. Imran, S. Wang, and F. M. F. Flaih, "DQ-voltage droop control and robust secondary restoration with eligibility to operate during communication failure in autonomous microgrid," *IEEE Access*, vol. 7, pp. 6353–6361, 2019.

[3] S. Zhang, C. Chen, L. Dong, Y. Li, J. Zhao, H. Nian, and L. Kong, "An enhanced droop control strategy for accurate reactive power sharing in islanded microgrids," in *Proc. IEEE Innov. Smart Grid Technol.-Asia (ISGT Asia)*, May 2019, pp. 2352–2356.

[4] T. V. Hoang and H.-H. Lee, "An adaptive virtual impedance control scheme to eliminate the reactive-power-sharing errors in an islanding meshed microgrid," *IEEE J. Emerg. Sel. Topics Power Electron.*, vol. 6, no. 2, pp. 966–976, Jun. 2018.

[5] Y. C. C. Wong, C. S. Lim, A. J. Cruden, M. D. Rotaru, and P. K. Ray, "A consensus-based adaptive virtual output impedance control scheme for reactive power sharing in meshed microgrids," in *Proc. IEEE Int. Conf. Power Electron., Smart Grid Renew. Energy (PESGRE)*, Jan. 2020, pp. 1–6.

[6] R. Heydari, T. Dragicevic, and F. Blaabjerg, "High-bandwidth secondary voltage and frequency control of VSC-based AC microgrid," *IEEE Trans. Power Electron.*, vol. 34, no. 11, pp. 11320–11331, Nov. 2019.

[7] W. Gu, G. Lou, W. Tan, and X. Yuan, "A nonlinear state estimator-based decentralized secondary voltage control scheme for autonomous microgrids," *IEEE Trans. Power Syst.*, vol. 32, no. 6, pp. 4794–4804, Nov. 2017.

[8] H. Zhang, S. Kim, Q. Sun, and J. Zhou, "Distributed adaptive virtual impedance control for accurate reactive power sharing based on consensus control in microgrids," *IEEE Trans. Smart Grid*, vol. 8, no. 4, pp. 1749–1761, Jul. 2017.

[9] J. Schiffer, T. Seel, J. Raisch, and T. Sezi, "Voltage stability and reactive power sharing in inverter-based microgrids with consensus-based distributed voltage control," *IEEE Trans. Control Syst. Technol.*, vol. 24, no. 1, pp. 96–109, Jan. 2016.

[10] H.-J. Yoo, T.-T. Nguyen, and H.-M. Kim, "Consensus-based distributed coordination control of hybrid AC/DC microgrids," *IEEE Trans. Sustain. Energy*, vol. 11, no. 2, pp. 629–639, Apr. 2020.

[11] Q. Shafiee, V. Nasirian, J. C. Vasquez, J. M. Guerrero, and A. Davoudi, "A multi-functional fully distributed control framework for AC microgrids," *IEEE Trans. Smart Grid*, vol. 9, no. 4, pp. 3247–3258, Jul. 2018.

[12] M. Shi, X. Chen, J. Zhou, Y. Chen, J. Wen, and H. He, "PI-consensus based distributed control of AC microgrids," *IEEE Trans. Power Syst.*, vol. 35, no. 3, pp. 2268–2278, May 2020.

[13] J. W. Simpson-Porco, Q. Shafiee, F. Dörfler, J. C. Vasquez, J. M. Guerrero, and F. Bullo, "Secondary frequency and voltage control of islanded microgrids via distributed averaging," *IEEE Trans. Ind. Electron.*, vol. 62, no. 11, pp. 7025–7038, Nov. 2015.

[14] J. Liu, J. Li, H. Song, A. Nawaz, and Y. Qu, "Nonlinear secondary voltage control of islanded microgrid via distributed consistency," *IEEE Trans. Energy Convers.*, vol. 35, no. 4, pp. 1964–1972, Dec. 2020.

[15] J. Lai, X. Lu, X. Li, and R.-L. Tang, "Distributed multiagent-oriented average control for voltage restoration and reactive power sharing of autonomous microgrids," *IEEE Access*, vol. 6, pp. 25551–25561, May 2018.

[16] X. Lu, X. Yu, J. Lai, Y. Wang, and J. M. Guerrero, "A novel distributed secondary coordination control approach for islanded microgrids," *IEEE Trans. Smart Grid*, vol. 9, no. 4, pp. 2726–2740, Jul. 2018.

[17] R. Han, L. Meng, G. Ferrari-Trecate, E. A. A. Coelho, J. C. Vasquez, and J. M. Guerrero, "Containment and consensus-based distributed coordination control to achieve bounded voltage and precise reactive power sharing in islanded AC microgrids," *IEEE Trans. Ind. Appl.*, vol. 53, no. 6, pp. 5187–5199, Nov. 2017.

[18] Y. Xu, Q. Guo, H. Sun, and Z. Fei, "Distributed discrete robust secondary cooperative control for islanded microgrids," *IEEE Trans. Smart Grid*, vol. 10, no. 4, pp. 3620–3629, Jul. 2019.

[19] X. Wu, C. Shen, and R. Iravani, "A distributed, cooperative frequency and voltage control for microgrids," *IEEE Trans. Smart Grid*, vol. 9, no. 4, pp. 2764–2776, Jul. 2018.

[20] A. Bidram, A. Davoudi, and F. L. Lewis, "A multiobjective distributed control framework for islanded AC microgrids," *IEEE Trans. Ind. Informat.*, vol. 10, no. 3, pp. 1785–1798, Aug. 2014.

[21] X. Wu, Y. Xu, X. Wu, J. He, J. M. Guerrero, C.-C. Liu, K. P. Schneider, and D. T. Ton, "A two-layer distributed cooperative control method for islanded networked microgrid systems," *IEEE Trans. Smart Grid*, vol. 11, no. 2, pp. 942–957, Mar. 2020.

[22] R. V. A. Neves, R. Q. Machado, V. A. Oliveira, X. Wang, and F. Blaabjerg, "Multitask fuzzy secondary controller for AC microgrid operating in stand-alone and grid-tied mode," *IEEE Trans. Smart Grid*, vol. 10, no. 5, pp. 5640–5649, Sep. 2019.

[23] A. Bidram, A. Davoudi, F. L. Lewis, and J. M. Guerrero, "Distributed cooperative secondary control of microgrids using feedback linearization," *IEEE Trans. Power Syst.*, vol. 28, no. 3, pp. 3462–3470, Aug. 2013.

[24] N. M. Dehkordi, N. Sadati, and M. Hamzeh, "Fully distributed cooperative secondary frequency and voltage control of islanded microgrids," *IEEE Trans. Energy Convers.*, vol. 32, no. 2, pp. 675–685, Jun. 2017.

[25] F. Guo, C. Wen, J. Mao, and Y. D. Song, "Distributed secondary voltage and frequency restoration control of droop-controlled inverter-based microgrids," *IEEE Trans. Ind. Electron.*, vol. 62, no. 7, pp. 4355–4364, Jul. 2015.

[26] M. Chen, X. Xiao, and J. M. Guerrero, "Secondary restoration control of islanded microgrids with a decentralized event-triggered strategy," *IEEE Trans. Ind. Informat.*, vol. 14, no. 9, pp. 3870–3880, Sep. 2018.

[27] Z. Afshar, M. Mollayousefi, S. M. T. Bathaee, M. T. Bina, and G. B. Gharehpetian, "A novel accurate power sharing method versus droop control in autonomous microgrids with critical loads," *IEEE Access*, vol. 7, pp. 89466–89474, Jul. 2019.

[28] F. Qiao and J. Ma, "Voltage/var control for hybrid distribution networks using decomposition-based multiobjective evolutionary algorithm," *IEEE Access*, vol. 8, pp. 12015–12025, Jan. 2020.

[29] X. Yang, Y. Du, J. Su, L. Chang, Y. Shi, and J. Lai, "An optimal secondary voltage control strategy for an islanded multibus microgrid," *IEEE J. Emerg. Sel. Topics Power Electron.*, vol. 4, no. 4, pp. 1236–1246, Dec. 2016.

[30] G. Agundis-Tinajero, N. L. D. Aldana, A. C. Luna, J. Segundo-Ramírez, N. Visairo-Cruz, J. M. Guerrero, and J. C. Vazquez, "Extended-optimal-power-flow-based hierarchical control for islanded AC microgrids," *IEEE Trans. Power Electron.*, vol. 34, no. 1, pp. 840–848, Jan. 2019.

[31] M. M. A. Abdelaziz, H. E. Farag, E. F. El-Saadany, and Y. A.-R. I. Mohamed, "A novel and generalized three-phase power flow algorithm for islanded microgrids using a Newton trust region method," *IEEE Trans. Power Syst.*, vol. 28, no. 1, pp. 190–201, Feb. 2013.

[32] F. Mumtaz, M. H. Syed, M. A. Hosani, and H. H. Zeineldin, "A novel approach to solve power flow for islanded microgrids using modified Newton Raphson with droop control of DG," *IEEE Trans. Sustain. Energy*, vol. 7, no. 2, pp. 493–503, Apr. 2016.

[33] A. La Bella, S. R. Cominesi, C. Sandroni, and R. Scattolini, "Hierarchical predictive control of microgrids in islanded operation," *IEEE Trans. Autom. Sci. Eng.*, vol. 14, no. 2, pp. 536–546, Apr. 2017.

[34] H. R. Baghaee, M. Mirsalim, and G. B. Gharehpetian, "Power calculation using RBF neural networks to improve power sharing of hierarchical control scheme in multi-DER microgrids," *IEEE J. Emerg. Sel. Topics Power Electron.*, vol. 4, no. 4, pp. 1217–1225, Dec. 2016.

[35] E. E. Pompodakis, G. C. Kryonidis, and M. C. Alexiadis, "A comprehensive load flow approach for grid-connected and islanded AC microgrids," *IEEE Trans. Power Syst.*, vol. 35, no. 2, pp. 1143–1155, Mar. 2020.

[36] J. Yang, N. Zhang, C. Kang, and Q. Xia, "A state-independent linear power flow model with accurate estimation of voltage magnitude," *IEEE Trans. Power Syst.*, vol. 32, no. 5, pp. 3607–3617, Sep. 2017.

[37] Y. Liu, N. Zhang, Y. Wang, J. Yang, and C. Kang, "Data-driven power flow linearization: A regression approach," *IEEE Trans. Smart Grid*, vol. 10, no. 3, pp. 2569–2580, May 2019.

[38] J. Machowski, J. W. Bialek, and J. R. Bumby, *Power System Dynamics: Stability and Control*, 2nd ed. West Sussex, U.K.: Wiley, 2008.

[39] Y. Liu, Y. Wang, N. Zhang, D. Lu, and C. Kang, "A data-driven approach to linearize power flow equations considering measurement noise," *IEEE Trans. Smart Grid*, vol. 11, no. 3, pp. 2576–2587, May 2020.

[40] D. Yu, J. Cao, and X. Li, "Review of power system linearization methods and a decoupled linear equivalent power flow model," in *Proc. Int. Conf. Electron. Technol. (ICET)*, May 2018, pp. 232–239.

[41] L. Wang, *Model Predictive Control System Design and Implementation Using MATLAB*. London, U.K.: Springer-Verlag, 2009.

[42] K. Dvijotham and D. K. Molzahn, "Error bounds on the DC power flow approximation: A convex relaxation approach," in *Proc. IEEE 55th Conf. Decis. Control (CDC)*, Dec. 2016, pp. 2411–2418.

[43] D. Van Hertem, J. Verboomen, K. Purchala, R. Belmans, and W. L. Kling, "Usefulness of DC power flow for active power flow analysis with flow controlling devices," in *Proc. 8th IEE Int. Conf. AC DC Power Transmiss. (ACDC)*, 2006, pp. 58–62.

[44] Y. Wang, H. Wu, H. Xu, Q. Li, and S. Liu, "A general fast power flow algorithm for transmission and distribution networks," *IEEE Access*, vol. 8, pp. 23284–23293, Feb. 2020.

[45] A. Bidram, V. Nasirian, A. Davoudi, and F. L. Lewis, "Control of AC microgrids," in *Cooperative Synchronization in Distributed Microgrid Control*. Cham, Switzerland: Springer, 2017, pp. 32–36.

[46] Y. C. C. Wong, C. S. Lim, M. D. Rotaru, A. Cruden, and K. Xin, "Reactive power sharing study of an islanded microgrid in DIgSILENT PowerFactory," in *Proc. 7th Int. Conf. Renew. Energy Res. Appl. (ICRERA)*, Oct. 2018, pp. 1–6.

[47] N. Pogaku, M. Prodanovic, and T. C. Green, "Modeling, analysis and testing of autonomous operation of an inverter-based microgrid," *IEEE Trans. Power Electron.*, vol. 22, no. 2, pp. 613–625, Mar. 2007.

[48] Z. Li, Z. Cheng, J. Liang, J. Si, L. Dong, and S. Li, "Distributed event-triggered secondary control for economic dispatch and frequency restoration control of droop-controlled AC microgrids," *IEEE Trans. Sustain. Energy*, vol. 11, no. 3, pp. 1938–1950, Jul. 2020.

[49] H. Lahiji, J. Mohammadi, F. B. Ajaei, and R. Boudreau, "Damping power oscillations in the inverter-dominated microgrid," in *Proc. IEEE Electr. Power Energy Conf. (EPEC)*, Oct. 2018, pp. 1–7.

[50] Y. Sun, X. Hou, J. Yang, H. Han, M. Su, and J. M. Guerrero, "New perspectives on droop control in AC microgrid," *IEEE Trans. Ind. Electron.*, vol. 64, no. 7, pp. 5741–5745, Jul. 2017.

**YI CHYN CASSANDRA WONG** (Student Member, IEEE) received the B.Eng. degree (Hons.) in electrical power engineering from Curtin University, Malaysia, in 2016. She is currently pursuing the split-site Ph.D. degree with the University of Southampton, U.K., and the University of Southampton Malaysia.

She was a Research Intern with the Experimental Power Grid Centre, Agency for Science, Technology and Research (A*STAR), Singapore, in 2017. Her research interests include power quality improvement, optimization control, and distributed cooperative control in microgrid.

**CHEE SHEN LIM** (Senior Member, IEEE) received the B.Eng. degree (Hons.) in electrical engineering from the University of Malaya, Malaysia, in 2009, and the joint-university Ph.D. degree in power electronics and drives from the University of Malaya and Liverpool John Moores University, U.K., in 2013.

He was a Research Scientist with the Experimental Power Grid Centre, A*STAR, Singapore, from 2013 to 2015. He joined the University of Southampton Malaysia, in November 2015, as an Assistant Professor of electrical and electronic engineering, and he is currently an Associate Professor. His research interests include advanced model predictive control design, multiphase motor drives, grid-connected converter control, and microgrid's hierarchical control. He serves as an Associate Editor for the *IET Electric Power Applications*.

**HUI HWANG GOH** (Senior Member, IEEE) received the B.Eng. degree (Hons.) in electrical engineering, the M.Eng. degree in electrical engineering, and the Ph.D. degree from Universiti Teknologi Malaysia (UTM), Johor, Malaysia, in 1998, 2002, and 2007, respectively.

He is currently a Professor of electrical engineering with the School of Electrical Engineering, Guangxi University, Nanning, China. His research interests include embedded power generation modeling and simulation, power quality studies, wavelet analysis, multi-criteria decision-making, renewable energies, and dynamic equivalent. He is a fellow of the Institution of Engineering and Technology (IET), U.K. He is also a fellow of the ASEAN Academy of Engineering and Technology (AAET) and the Chinese Society of Electrical Engineering (CSEE). He is a Chartered Engineer under the Engineering Council United Kingdom (ECUK). He is a Professional Engineer under the Board of Engineers, Malaysia (BEM).

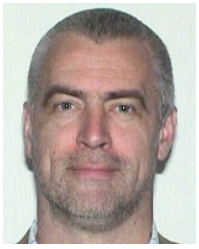

**ANDREW CRUDEN** received the B.Eng., M.Sc., and Ph.D. degrees in electronic and electrical engineering from the University of Strathclyde, Glasgow, U.K., in 1989, 1990, and 1998, respectively.

He is currently the Associate Dean (Infrastructure) of the Faculty of Engineering and Physical Sciences (FEPS) and a Professor of energy technology with the University of Southampton, U.K. He has significant experience in the field of energy storage and electric vehicles, covering vehicle-to-grid (V2G), new battery technologies, such as aluminium-ion cells, and flow cells, such as soluble lead flow battery. He has previously worked in fuel cell technology and condition monitoring of wind turbines. He is a member of the Training and Diversity Panel of the U.K.'s Faraday Institution and the Co-Director of the EPSRC Centre for Doctoral Training (CDT) in energy storage and its applications.

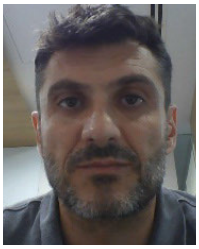

**MIHAI DRAGOS ROTARU** (Member, IEEE) received the B.Eng. and M.Sc. degrees in electrical engineering from the Technical University of Cluj-Napoca, Romania, in 1996 and 1997, respectively, and the Ph.D. degree in electrical engineering from the University of Southampton, U.K., in 2001.

He was an Assistant Professor then an Associate Professor with the School of Electronics and Computer Science, University of Southampton, from 2007 to 2019. He served as the Electrical and Electronic Engineering Program Leader for the University of Southampton Malaysia, from 2013 to 2019. He is currently a Senior Scientist with the Institute of Microelectronics, A*STAR, Singapore. His research interests and expertise include simulation and modeling of complex applied electromagnetic problems.

**XIN KONG** received the B.Eng. and M.Eng. degrees in electrical engineering from Xi'an Jiaotong University, China, in 1994 and 1997, respectively, and the Ph.D. degree in electrical engineering from the National University of Singapore, Singapore, in 2009.

She is currently a Principal Research Scientist and the Deputy Program Director of the Energy Research Institute at NTU (ERI@N), Nanyang Technological University, Singapore. Her research interests include modern power system modeling and analysis, renewable energy integration, distributed microgrid control, and power electronic design and control for grid application.